
Does a Teleconnection between Quantum States account for Missing Mass, Galaxy Ageing, Lensing Anomalies, Supernova Redshift, MOND, and Pioneer Blueshift?

Charles Francis

104b Cherry Hinton Rd, Cambridge CB1 7AJ

Submitted: 26/8/06

Abstract:

Empirical implications of a teleparallel displacement of momentum between initial and final quantum states, using conformally flat *quantum coordinates* are investigated. An exact formulation is possible in an FRW cosmology in which cosmological redshift is given by $1 + z = a_0^2/a^2(t)$. This is consistent with current observation for a universe expanding at half the rate and twice as old as indicated by a linear law, and, in consequence, requiring a quarter of the critical density for closure. A no CDM teleconnection model resolves inconsistencies between galactic profiles found from lensing data, rotation curves and analytic models of galaxy evolution. The teleconnection model favours a closed no Λ cosmology. After rescaling Ω so that $\Omega = 1$ is critical density, for 225 supernovae, the best fit teleconnection no Λ model with $\Omega = 1.89$ is marginally preferred to the best fit standard flat space Λ model with $\Omega = 0.284$. It will require many observations of supernovae at $z > 1.5$ to eliminate either the standard or teleconnection magnitude-redshift relation. In quantum coordinates the anomalous Pioneer blueshift and the flattening of galaxies' rotation curves appear as optical effects, not as modifications to classical motions. An exact form of Milgrom's phenomenological law (MOND) is shown.

Key Words: Cosmology: cosmological parameters, theory, dark matter, distance scale; Galaxies: haloes, kinematics and dynamics.

PACS: 04.80.Cc, 95.30.Sf; 98.80.Jk, 98.80.Qc

1 Background

There is growing concern in Cosmology about unexplained empirical phenomena. The standard model of accelerating expansion is successful in matching parameters to observation, but, while there is no true reconciliation between general relativity and quantum mechanics, science should remain open to the prospect that these phenomena may have some deep underlying reason in new physics. The concept of a teleconnection arose from theoretical research into the foundations of quantum theory (Francis, 2006), but the essential tests of a new model of physics are whether the model is consistent with data, whether it gives accounts of observed phenomena which the standard model has been unable to explain, and whether it makes predictions about future tests which further distinguish it from the standard model.

It is known on theoretical grounds that new physics is required to reconcile general relativity and quantum theory (e.g Dirac, 1964, Rovelli 2004) and Eppley and Hannah (1977) showed the necessity of a quantum treatment of gravity. A new model of physics should adhere to fundamental principles such as the cosmological principle, the special and general principles of relativity, the uncertainty principle and the principle of superposition. This paper carries out a preliminary investigation of the empirical implications of a modification to gen-

eral relativity adhering to these fundamental principles. Standard general relativity and quantum mechanics are assumed, except that the affine connection is replaced and wave functions are defined using *quantum coordinates*, not in curved spacetime. The tests described here could have falsified the model, but if anything the reverse is the case and an initial analysis of current astronomical data is consistent with a closed universe and no cold dark matter or cosmological constant, but with no apparent timescale problem (table 1).

Einstein (1930) suggested that the affine connection used in general relativity might be replaced with a teleparallel connection. Such a replacement can be motivated in the orthodox interpretation of quantum mechanics; if it does not make sense to talk of position between measurements then it also makes no sense to talk of geodesic motion of a photon emitted from a distant star and detected on Earth. Individual detection of photons from distant stars suggests that quantum theoretical effects may come into play. If this is the case we cannot be certain of the analysis of redshift without first having a rigorous formulation of quantum motions in curved space time. In general relativity it is assumed that photon momentum is parallel transported through large distances, but wave motion and collapse in curved space-time is problematic and fundamentally distinct from geodesic motion. It would imply that a photon of precise momentum at time of emission does not have precise momentum at absorption. Here we consider the wave function in a quantum formulation, as a probabilistic relationship between an initial and a final state, respectively the emission and detection of a photon, in which momentum is precisely conserved after taking into account redshift. The connection is defined between the remote coordinate systems used to describe these states and will be called a *teleconnection*.

A heuristic description of the teleconnection is given in section 2. For this purpose a closed universe will be discussed. Other models are possible, but this simple model is consistent with observation and should be sufficient to understand the empirical tests described in sections 3 to 9. A formal treatment is deferred to appendix A, showing that the teleconnection can be consistently defined in an FRW cosmology, that the prescription reduces to the standard affine connection in the classical correspondence, and that geodesic motion obtains for classical particles and for a beam of light.

The modification has a number of testable implications. A revised relationship between redshift and age offers the prospect of a reconciliation between observation and galaxy evolution models (section 3). The magnitude-redshift relation has been analysed using data sets from Riess (2004) and Astier (2005), and the teleconnection model gives marginally better fits

Table 1: Properties Compared

Model	Standard ($\Omega_k = 0$)	Teleconnection ($\Lambda = 0$)
Expansion rate	$\dot{a}/a = H$	$\dot{a}/a = H/2$
Critical density ($\Omega = 1$)	$3H^2/8\pi G$	$3H^2/32\pi G$
Topology	Open	Closed
Ω	0.28	1.89
Ω_B	0.025~0.05	0.1~0.2
Current age	~14 Gyr	~17 Gyr
Age at $z = 6$	~0.7 Gyr	~4.5 Gyr
CDM haloes	inconsistent	absent
Pioneer blueshift	unexplained	$a_p = H_0 c$
MOND	CDM	$a_M = H_0 c/8$
Wave motion	curved space?	flat space
Classical motion	geodesic	geodesic

for these data sets both individually and combined (section 5). There is no consistent standard model for CDM haloes (section 4) or explanation for either Pioneer blueshift (section 6) or MOND (section 7), but the teleconnection models the flattening of galaxies' rotation curves and Pioneer blueshift, without requiring either a change to Newtonian dynamics or galactic haloes. In the instance of galactic rotation curves testing has been done, not through direct statistical analysis, but by deriving a general law (MOND) already established from statistical analysis. Attention will be drawn to possible further tests for which the analysis is subtle and goes beyond the scope of this paper.

2 The Teleconnection

This is not a teleparallel theory using the Weitzenböck connection (see e.g. Arcos and Pereira, 2004). The teleconnection applies between initial and final states in the quantum theory. It does not apply when there is an intermediate measured state. In the classical correspondence, when continuous measurement is possible in principle, torsion will be removed and gravity will be described by curvature, as is normal in general relativity. As in general relativity there is no local meaning to expansion because length is defined locally, by an empirical procedure using local matter. To talk about expansion we have to compare a length scale defined here and now, using here and now clocks and rulers, with a length scale defined at some time in the past. In practice we can do this by studying light from the past and analysing redshift *provided* that we know how light behaves. The definition of a teleconnection assumes that if momentum has a precise value at one place and time then it also has a precise value other places and times and is empirically justified in so far as observation yields precise values for cosmological redshift after allowing for dispersion due to dust or other known factors. This is a fundamental assumption in this model, of equal importance to the assumption of the constancy of the speed of light in special relativity. Like that assumption, if it were dropped we would be left, not with a different theory, but with no known consistent theory.

Let Alf be an observer on a space craft or a distant planet, and let Beth be an observer on Earth, such that Alf can signal to Beth. At the time of emission of a photon passing from Alf to Beth, Alf defines synchronous co-ordinates in 3 dimensions at constant cosmic time t , using proper distance as the radial coordinate (figure 1). In a closed cosmos the universe can be mapped onto a finite space, which will be called *Alf's map*. Beth defines *Beth's map* in exactly the same way, to the same scale, at the time of detection of the photon, cosmic time t_0 . For a closed universe in three dimensions Alf's and Beth's maps are each contained in a sphere. Let $a(t)$ be the scale factor and let $a_0 = a(t_0)$. If the universe expands during the time of travel of the photon from Alf to Beth, then Beth's map is larger than Alf's map by a factor $a_0/a(t)$.

Alf and Beth each define rigged Hilbert spaces spanned by position states, $|x\rangle$, at their own cosmic time, and, using the Euclidean metric at the origin of their own coordinates, they formally define plane wave states by

$$|p\rangle = \left(\frac{1}{2\pi}\right)^{3/2} \int_{-\pi a}^{\pi a} d^3x e^{ix \cdot p} |x\rangle. \quad (2.1)$$

Although a wave is usually considered as a function on space, $\langle x|p\rangle$ is strictly a function of the coordinate system, and is defined at the origin for each observer; it will be observed that Alf's and Beth's formulations differ by a scale factor. This reflects the orthodox interpretation in which wave functions do not represent a physical wave property, and are merely used by an observer to calculate probabilities.

A connection is required to enable the definition of an inner product between states in Alf's and Beth's Hilbert spaces and thereby formulate a quantum theory of the motion of a photon

from Alf to Beth from an initial state $|f(t)\rangle$ at Alf's cosmic time to a final state $|f(t_0)\rangle$ at Beth's cosmic time. As Alf's and Beth's Hilbert spaces are defined at remote origins, it is called a teleconnection. To make a teleconnection, Beth first enlarges Alf's map by the factor $a_0/a(t)$. Likewise Alf reduces Beth's map. Alf and Beth now define four dimensional maps by considering all the times and positions where the other might be, with time scaled so that light is shown at a constant angle necessary to plane wave motions (figure 3). These are Penrose diagrams in each time-radial plane. The teleconnection is defined so that photon momentum is represented by a vector of equal magnitude and direction on Beth's map and on Alf's enlarged map (figure 2). An inner product between states in Alf's and Beth's Hilbert spaces is defined by replacing x and p with *coordinate space vectors* \bar{x}, \bar{p} where $\bar{x} = x$ and $\bar{p} = p$. Coordinate space vectors are invariant under translation in the time-radial plane in coordinate space, as shown by the red arrow in figure 2, and are related to physical vectors by inverting scaling distortions in the maps using (A1.3). (2.1) is thus replaced by

$$|\bar{p}\rangle = \left(\frac{1}{2\pi}\right)^{3/2} \int_{-\pi}^{\pi} d^3\bar{x} e^{i\bar{x}\cdot\bar{p}} |\bar{x}\rangle. \quad (2.2)$$

and, for a closed FRW cosmology, there is a precise formulation of quantum mechanics in which the wave function is invertible

$$\langle\bar{x}|f\rangle = \left(\frac{1}{2\pi}\right)^{3/2} \int_{-\pi}^{\pi} d^3p \langle\bar{p}|f\rangle e^{-i\bar{x}\cdot\bar{p}}. \quad (2.3)$$

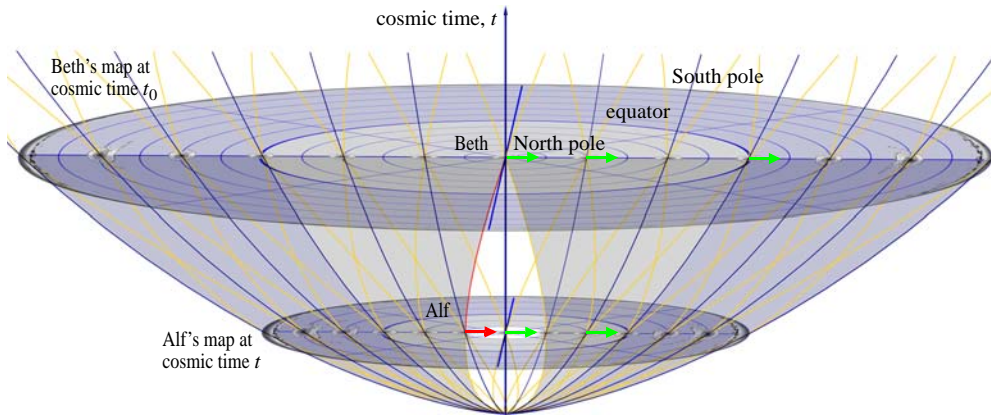


Figure 1: Alf and Beth's maps at constant cosmic time with radial coordinate equal to proper distance. Alf and Beth are here drawn in different galaxies. For convenience Beth's galaxy is taken as the origin of both maps. One dimension is suppressed, so the maps are spherical in three dimensional space. Identical galaxies are shown on geodesics emanating from the big bang in the $x-t$ plane. As drawn each galaxy has the same radial dimension but the galaxies acquire an increasing angular stretch towards the edge of the map. These scaling distortions are physically meaningless and can be removed by embedding the $x-y$ plane onto the surface of a sphere with Beth at the North pole. Thus local geometrical properties are everywhere the same in accordance with the cosmological principle. The circles on the maps correspond to lines of latitude at 15° and 30° intervals for Beth's and Alf's respective maps. The region corresponding to the Southern hemisphere, shaded blue, appears outside the Northern hemisphere. The outermost circumference is infinitely stretched and represents a point, the South pole. The galaxy at the South pole is so stretched that it surrounds the map. In the diagram the universe doubles in size between Alf's and Beth's cosmic time, at which point it is at half maximum expansion. The path of light is shown in yellow, with the signal from Alf to Beth shown in red. The region outside Beth's past light cone is shaded grey. A space-like radial vector has the same apparent and proper length at any point (green). In his own coordinates Alf scales a red coordinate space vector to be equal to the green physical vector.

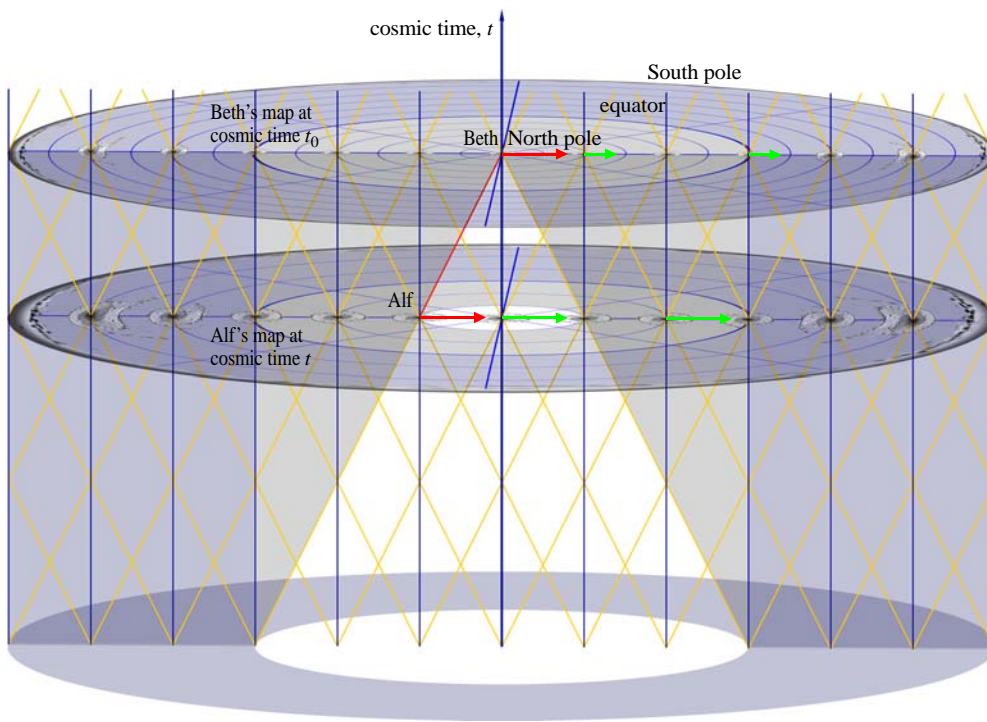


Figure 2: Beth's map of space time. The scale of Alf's map is doubled so that it is the same size as Beth's. Both the red coordinate space vector and the green physical vector on Alf's map appear twice as long in these coordinates. The time axis is also rescaled, being stretched downwards by greater amounts approaching the big bang, so that light is shown at a constant angle. This condition is necessary and sufficient for radial plane wave motions, defined using coordinate space vectors which have the same apparent length everywhere. Since the apparent length of a coordinate space vector (red) remains the same under teleparallel displacement from Alf to Beth, its real length doubles.

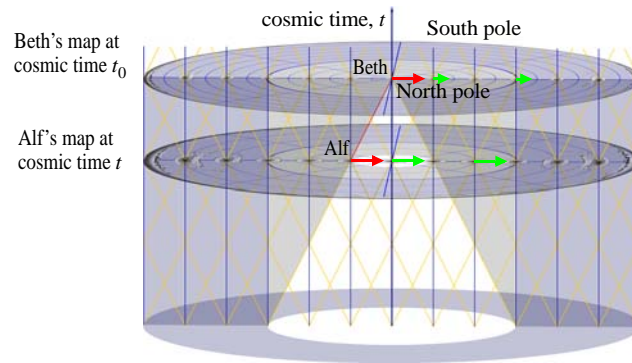


Figure 3: Alf's map of space-time is found by halving the scale of Beth's map. Beth formulates quantum theory on figure 1, while Alf formulates it on figure 2. So Beth sees a net factor of four in the wavelength of an e.m. signal sent from Alf to Beth, and the redshift is $z = 3$, not $z = 1$ as would be the case in the standard model.

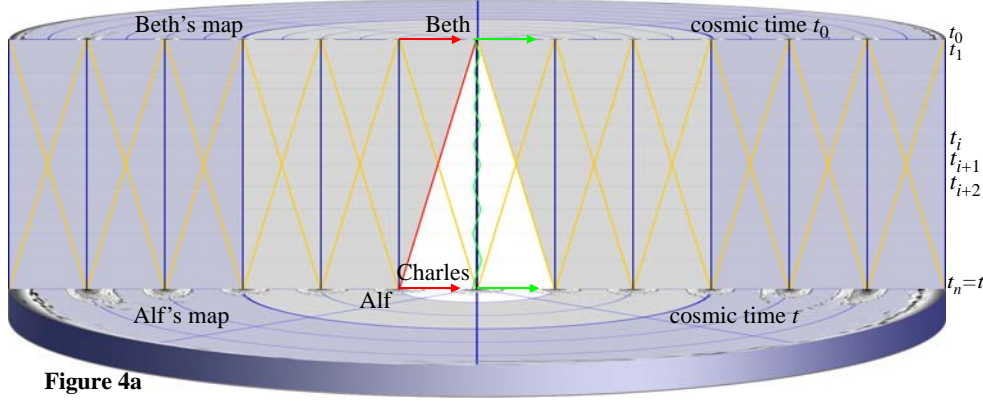


Figure 4a

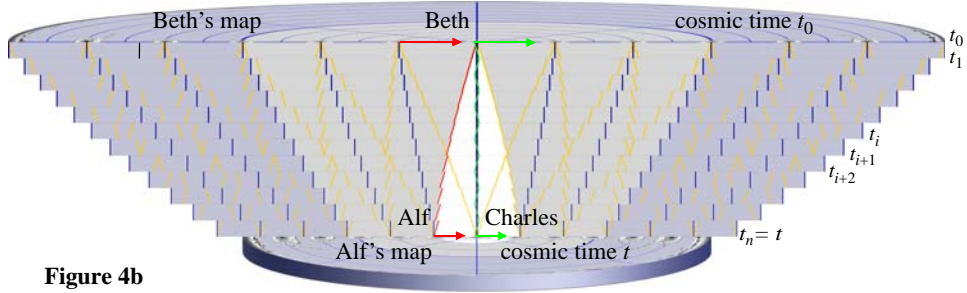


Figure 4b

Figure 4: In the classical correspondence it is possible to define the state on synchronous spatial surfaces at constant cosmic times t_i separated by a small interval. The state at any instant, t_i , may be regarded as an initial quantum state. The state at the next instant t_{i+1} may be regarded as a final state, which, after rescaling, becomes the initial state for the next part of the motion. Time evolution is described as a series of quantum steps, $\langle f(t_{i+1}) | f(t_i) \rangle$. With each rescaling of coordinates between steps, momentum is renormalised such that, at each instant t_i , conservation of momentum is preserved and the non-linearity of time seen in figure 4a is removed. In the limit, $\forall i = 1, \dots, n, t_{i+1} - t_i \rightarrow 0$, figure 1 is restored. Thus, if Beth's ancestor, Charles, had set up a trapped signal (green) in a laboratory on Beth's planet, such that its wavelength could be measured at any time, then the classical linear redshift law found from the affine connection will be measured.

In practice Beth can compare the scale of her map to that of Alf's map by studying red shift. There are two scaling effects. First Alf's map has been enlarged by a factor $a_0/a(t)$. In addition, the scaling on the map changes from one point to another, giving another factor $a_0/a(t)$ from (A1.3). Thus, the model predicts a net factor for cosmological redshift which varies with the square of the expansion parameter:

$$1 + z = a_0^2/a^2. \quad (2.4)$$

(2.4) applies to a quantum motion between an initial state, $|f(t)\rangle$, at time t , and a final state, $|f(t_0)\rangle$, at time t_0 , when it is not meaningful to describe the intervening state in terms of measured physical quantities. In the classical correspondence time is taken as a continuous variable and motion may be described as a sequence of measured states $|f(t_i)\rangle$ at instances $t_i \in T$ for $i = 1, \dots, n$ such that $\forall i, 0 < t_i - t_{i+1} < \chi$ in the limit in which χ tends to zero. The state at any instant may be regarded as an initial state, and the state at the next instant may be regarded as a final state for that part of the motion. The final state then becomes the initial state for the next part of the motion. At each instant t_i the coordinate system must be rescaled such that the quantum theory is defined on the torus $(-\pi, \pi)^3$ (figure 4). The paths of light and of the gal-

axies become continuous in the limit $\chi \rightarrow 0$, in which figure 1 is recovered. We require that momentum is conserved at each instant, i.e. that the momentum space wave function is unchanged when a final state is reinterpreted as an initial state. Momentum must be renormalised upon rescaling, which requires a factor $a(t_{i+1})/a(t_i)$. It follows that momentum is parallel displaced from t_{i+1} to t_i and that (2.4) is replaced with the usual linear law

$$1 + z = a_0/a. \quad (2.5)$$

Thus, in the classical correspondence, the teleconnection reduces to a Riemann affine connection.

3 Cosmological Redshift

When light is received from a distant object cosmological redshift is given by (2.4). For small r

$$1 + z \approx 1 + 2r\dot{a}/a. \quad (3.1)$$

Thus coordinates in which radial distance from Earth is calculated from redshift exhibit a stretch of factor half in the radial direction. Using (A1.3), the radial component of the coordinate space position vector of an object at radius r is $\bar{r} = 2r$. The time taken for a pulse of light at this distance to traverse a small angular distance $d\theta$ is $\bar{r}d\theta = rd\theta$. So there is a stretch of factor two in the angular directions (this gives 4π in a circle, which may cast light on fermion phase under rotation). Thus the metric, (A3.2), for quantum coordinates is:

$$ds^2 = a^2(4(dt^2 - d\rho^2) - \frac{1}{4}f^2(\rho)(d\theta^2 + \sin^2\theta d\phi^2)). \quad (3.2)$$

Definition: *Hubble's constant, $H \equiv 2\dot{a}/a$, is read from (3.1).*

It follows immediately that the rate of expansion of the universe is half that predicted by the standard model, the universe is twice as old as would be indicated by a linear law, critical density for closure is a quarter of the standard value, and that there is no apparent timescale problem for a closed FRW universe with greater than critical density and zero cosmological constant.

If observations at high red shift had revealed the expected activity of the early universe it would have falsified the square red shift law; in fact it receives support from the observation of mature galaxies at $z = 1.4$ and greater (e.g. Mullis et al., 2005; Doherty et al 2005, and references cited therein). As described by Glazebrook (2004), there is poor agreement between current theoretical models of galaxy evolution and empirical data. To explain this it has been suggested (e.g. Cimatti et. al, 2004) that the theoretical models may be inaccurate. This model presents an alternative, that a square redshift law means we have to revise the ages of red galaxies. A value of Hubble's constant $h = 0.72$ places an upper bound on the age of the universe of eighteen billion years; at redshift 6 the universe would have been about 4.5 billion years old. The accelerations of galaxies in clusters are in the MONDian regime, and after revising the age-redshift relation, there is neither immediate evidence that CDM is necessary to explain galaxy evolution, nor strong reason to suppose that galactic evolution models are inaccurate at the resolutions and step sizes available with today's supercomputers. A detailed study is required to assess consistency between observation and theory, but this model appears to alleviate the difficulties. Hopefully future observation and analysis will be conclusive.

4 Lensing

The teleconnection model predicts geodesic motion for a classical ray of light so that there is no change in the prediction of bending of light around a body such as the Sun, which has known mass and for which distance can be determined by direct measurement. The analysis is quite different for a lens whose distance is determined from redshift. In this case the bending

of light by the lens must be described using quantum coordinates, as given by (3.2) and seen in figure 5. Lensing is affected in two principal ways in the teleconnection model: first, in the absence of a CDM halo, lower galactic masses reduce lensing; second the use of quantum coordinates quadruples the angle of deflection as compared to standard general relativity.

Zhao et al. (2006) tested lensing in Beckenstein’s relativistic MOND (TeVeS), and concluded that lensing may be a good test for CDM theories. The problem for standard no CDM theories is that, because of the lower galactic masses it is difficult to account for the amount of lensing in all cases. Zhao et al. found that “TeVeS succeeds in providing an alternative to general relativity in some lensing contexts; however, it faces significant challenges when confronted with particular galaxy lens systems”. However, the empirical determination of the mass of the lensing galaxy is not sufficiently precise to eliminate it for all choices of parameters. Each observed lens requires careful analysis, but given that the teleconnection model predicts a substantially greater angle of deflection than TeVeS it appears unlikely that the determination of lens masses will provide a definitive test at the current level of accuracy of observation.

A clearer test may be the analysis of the profile of the halo. There is now a substantial literature on lensing profiles indicating that the standard CDM model is not consistent. According to evolutionary models dark matter halos should have steep central density cusps (e.g., Navarro, Frenk, & White 1997) but they appear not to (e.g., de Blok, Bosma, & McGaugh 2003; Swaters et al. 2003). In a survey of about 3000 galaxies, Biviano & Salucci (2006) find that X-ray determination of the baryonic component of dark matter halos fits evolutionary models, but subhalo components do not. Martel and Shapiro (2003) have examined the profile of lenses for a number of evolutionary models. While they find quantitative fits for many properties, they find that the models do not correctly reproduce the central region. Park and Ferguson (2003) studied the lensing produced by Burkert halos and found, “For the scaling relation that provides the best fits to spiral-galaxy rotation curve data, Burkert halos will not produce strong lensing, even if this scaling relation extends up to masses of galaxy clusters. Tests of a simple model of an exponential stellar disk superimposed on a Burkert-profile halo demonstrate that strong lensing is unlikely without an additional concentration of mass in the galaxy center (e.g. a bulge)”.

Power et al (2003) also comment on discrepancies between analytic models and halo distribution required by galaxy rotation curves. In particular they state “there is no well defined value for the central density of the dark matter, which can in principle climb to arbitrarily large values near the centre”. Of this result they say “there have been a number of reports in the lit-

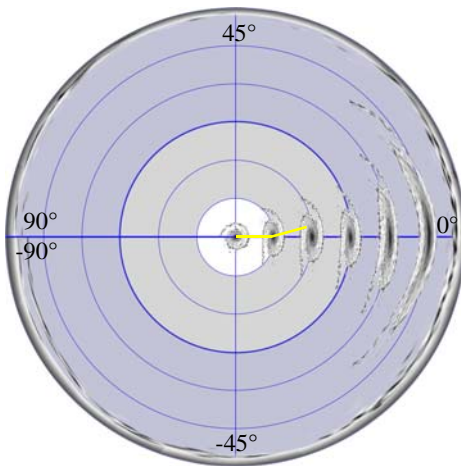


Figure 5: Alf’s map in quantum coordinates. Quantum coordinates apply to wave functions and are not directly measured, except in the direction of the positive x -axis, i.e. the direction in which one is actually looking at an incoming photon. Radial distance is halved, but angular distances are doubled. This increases the deflection angle by a factor of four as compared to other no-CDM models. The diagram is discontinuous on the negative x -axis and has two parts. This applies to deflection of light by distant galaxies, but not to deflection around the sun which can be described classically in the solar reference frame (section 6)

erature arguing that the shape of the rotation curves of many disk galaxies rules out steeply divergent dark matter density profiles” and conclude that it “may signal a genuine crisis for the CDM paradigm on small scales”. On the other side of the debate, Milgrom and Sanders (2005) found halo properties in Ursa Major Galaxies consistent with MOND predictions, and in a one study for which a particularly good analysis is possible, Wayth et al. (2005) found that, for the optical Einstein ring gravitational lens ER 0047-2808, lensing is consistent with a halo of the same mass distribution as the galaxy itself. This result is not consistent with either the halo distribution required to produce galactic rotation curves, or with evolutionary halo models. It is, of course, trivially consistent with both in a no CDM model.

5 Cosmological Parameters

The interpretation of redshift alters cosmological parameters but otherwise leave the established equations of general relativity unchanged. Friedmann’s equation is

$$\dot{a}^2 = \frac{8}{3}\pi G\rho_0 a_0^3/a + \frac{1}{3}\Lambda a^2 - k. \quad (5.1)$$

Normalising so that $\Omega = 1$ is critical density Ω takes on four times its standard value:

$$\Omega = 32\pi G\rho_0/3H_0^2, \quad \Omega_k = -4k/H_0^2 a_0^2, \quad \text{and} \quad \Omega_\Lambda = 4\Lambda/3H_0^2, \quad (5.2)$$

where $k = -1, 0, 1$. Then Friedmann’s equation, (5.1), is,

$$\dot{a}/a = \frac{1}{2}H_0(\Omega(1+z)^{3/2} + \Omega_k(1+z) + \Omega_\Lambda)^{1/2}, \quad (5.3)$$

requiring that $\Omega + \Omega_k + \Omega_\Lambda = 1$.

Definition: Let the deceleration parameter be:

$$q \equiv -a\ddot{a}/\dot{a}^2 = -4\ddot{a}/aH^2. \quad (5.4)$$

Differentiate Friedmann’s equation:

$$\ddot{a}/a = -\frac{4}{3}\pi G\rho_0 a_0^3/a^3 + \frac{1}{3}\Lambda = -\frac{4}{3}\pi G\rho_0(1+z)^{3/2} + \frac{1}{3}\Lambda. \quad (5.5)$$

Let $H_0 = H(t_0)$, $a_0 = a(t_0)$ and $q_0 = q(t_0)$. From (5.2) and (5.5),

$$q_0 = \frac{\Omega}{2} - \Omega_\Lambda. \quad (5.6)$$

The coordinate distance from emission at time t_e to detection at time t_0 is

$$\rho = \int_{t_e}^{t_0} \frac{1}{a} dt = \int_{a_e}^{a_0} \frac{1}{2a^2 \dot{a}} d(a^2) = \int_0^z \frac{k\Omega_k^{1/2}(1+z)^{3/2}}{2(\Omega(1+z)^{3/2} + \Omega_k(1+z) + \Omega_\Lambda)^{1/2}} dz \quad (5.7)$$

The angular size distance is $a_0 \sin 2\rho$. The determination of luminosity distance now proceeds as in the standard model, observing that energy and rate of photon emission are shifted by $1+z$, as is standard. Thus luminosity distance is

$$d_L = \frac{c(1+z)}{H_0\Omega_k^{1/2}} \sin 2\rho = \frac{c(1+z)}{H_0\Omega_k^{1/2}} \sin \int_0^z \frac{k\Omega_k^{1/2}(1+z)^{3/2}}{(\Omega(1+z)^{3/2} + \Omega_k(1+z) + \Omega_\Lambda)^{1/2}} dz \quad (5.8)$$

The predicted distance modulus is $\mu = 5 \log d_L + 25$. Quantrix modeller has been used to run χ^2 tests on this relation for the Riess (2004) and Astier (2005) data sets. For the Astier data there are 115 degrees of freedom, excluding two outliers removed by Astier. Astier minimised with respect to four variables, Ω , M , α and β . This preliminary analysis used the optimum values of α and β found by Astier for the standard fit, and minimised with respect only to Ω and M . This means that χ^2 may be above the minimum for the teleconnection fit, but as the curves are very close throughout the data range it is unlikely that varying α and β will greatly affect the result. The best fit flat space standard model was $\Omega_s = 0.261$ with $\chi^2 = 113.6$. For the teleconnection flat space Λ model the best fit was $\Omega = 1.55$ with $\chi^2 = 117.1$, and for the $\Lambda = 0$ model it was $\Omega = 1.85$, $\chi^2 = 113.4$.

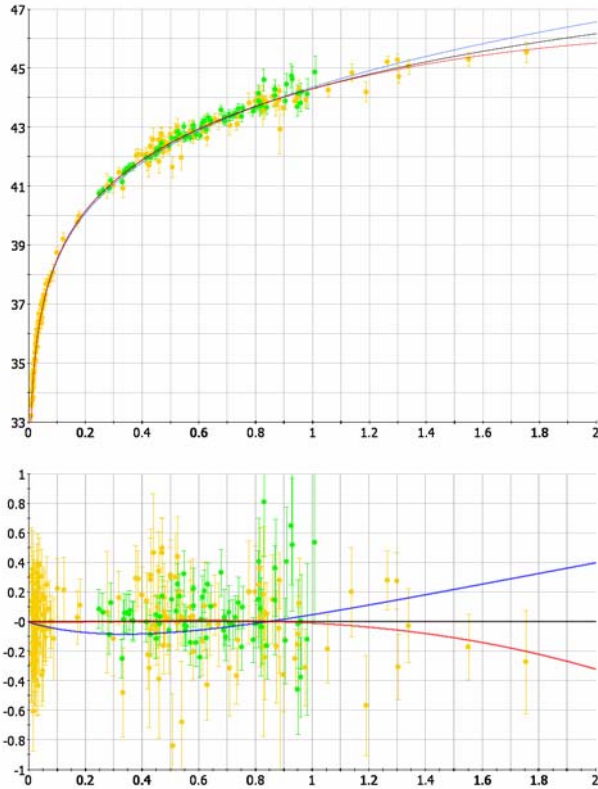


Figure 6: Hubble diagram with residuals to the best fit standard flat space Λ model with 225 dof; 154 supernovae from the Riess gold set in orange and 71 SNLS supernovae in green, corrected for the choice of Hubble’s constant (Astier uses many of the same supernovae as Riess in the near set). The best fit standard flat space Λ model (black) has $\Omega_s = 0.284$, $\chi^2 = 212.5$. The best fit teleconnection flat space model (blue) has $\Omega = 1.64$, $\chi^2 = 236.7$ (red). The best fit teleconnection no Λ model (red) has $\Omega = 1.89$ and $\chi^2 = 210.8$.

Three outliers were removed from the Riess gold set, one well beyond 3σ , and the other two beyond 2.75σ . These outliers all lie below the curve and are not representative of the population. Removal of outliers reduces χ^2 but makes little difference to the prediction for Ω . The lensing correction to SN1997ff was left in the fits for both models, as it is thought that lensing under the teleconnection model is similar to that of the standard model. The correction makes very little difference to the predictions for Ω or to χ^2 . For 154 dof the best fit with the standard model is $\Omega_s = 0.295$ with $\chi^2 = 151.3$. The best fit with the teleconnection flat space Λ model is $\Omega = 1.72$ with $\chi^2 = 171.7$, and the best fit no Λ model is $\Omega = 1.90$ with $\chi^2 = 150.0$. The Λ model is not eliminated by these fits. It is notable that for both data sets the teleconnection no Λ model is marginally preferred to the standard model and that there is a good degree of agreement in the predicted values of Ω for this model. There are substantial measurement difficulties at high z and current searches like SNLS and ESSENCE are directed at finding SN with $z < 1$. As seen from the residuals plot, figure 6, to eliminate either the teleconnection or the standard model it will be necessary to collect systematically a substantial body of observations at $z > 1.5$ and to rigorously analyse them to eliminate possible systematics. We may eagerly await the results of the SNAP mission, currently in the design stage.

6 Anomalous Pioneer Blueshift

For some years the Pioneer spacecraft sent back Doppler information interpreted as an anomalous acceleration toward the sun (Anderson et al., 2002). Turyshev et al. (2006) found “The Pioneer 11 data also indicated that the anomaly ... appears to be amplified (or turned on) at a distance of ~ 10 A.U. from the Sun. This is approximately when the craft flew by Saturn and entered an hyperbolic, escape trajectory”. Although what is measured is blueshift, JPL

expressed their result in the form of an equivalent classical acceleration, $a_p = 8.74 \pm 1.33 \times 10^{-8} \text{cms}^{-2}$. A future test is planned which will determine whether the acceleration is toward the Sun, toward the Earth, in the direction of motion of the craft, or along the spin axis (Nieto and Turyshev 2004). This information may also be discovered from reanalysis of the archive of Pioneer transmissions (Turyshev et al, 2006).

No accepted explanation has been given for the anomalous blueshift, but using the teleconnection there is an argument that it is as an effect of expansion when quantum coordinates are used to model transmissions between Earth and Pioneer. If this explanation is correct then, consistent with NASA's findings, there is no corresponding classical acceleration and Pioneer is on precisely the expected Newtonian path. The prediction is for a shift in Doppler measurements using signals with an effective Doppler frequency above a critical frequency, f_c , where f_c depends the accuracy of measurement. This is sensible in an orthodox interpretation of quantum mechanics in which the wave function is merely a mathematical device for the prediction of results, not a physical wave in space. Since accuracy of measurement depends on distance from the detector, or measurement apparatus, there is a critical distance, $\Delta = \Delta(f)$, above which the anomalous shift will be found in measurements at effective Doppler frequency f . For distances close to Δ we do not anticipate a clear measurement of the shift. In practice for distances less than the orbit of Saturn the anomalous acceleration is drowned by solar pressure which is neither constant nor easy to determine with great accuracy.

In standard general relativity, recession velocities due to cosmological expansion with $\dot{a}/a = H_0$ are precisely equal to the Doppler shift when expansion is viewed as motion in a fixed local reference frame. With the teleconnection the same shift corresponds to only half the recession velocity. It follows that in a fixed local frame there is a disparity between Doppler velocities and local motion for an object moving with the cosmic fluid. This disparity can be treated by a coordinate transform. For quantum coordinates with metric given by (3.2) the time coordinate obeys (A3.4), and exhibits acceleration with respect to proper time. Anderson remarks that the blueshift is equivalent to an "acceleration in time" equal to the Hubble constant, but rejects acceleration in time because, using conventional physics, it is incompatible with ranging data (Anderson, section XI.D). This is as expected in the teleconnection model since acceleration in time applies to quantum coordinates but not to physical, measured, time as used in radar. Acceleration in time is seen in figure 4a, in which discs of constant proper time become less deep as quantum time increases. The value of the acceleration in time is $H_0/2$ but blueshift is doubled in (3.1). The equivalent acceleration, $a_p = H_0 c$, is consistent with recent determinations of Hubble's constant. In the absence of a fully rigorous treatment of quantum coordinates in the presence of a gravitating body is not clear whether the direction of simulated acceleration is toward the origin of coordinates, i.e. the Sun, but it seems more natural that it should be in the direction travelled by the signal from Pioneer, i.e. towards the detector on Earth.

Within a locally defined reference frame it may be assumed that there is a continuous foliation of synchronous slices in which the path of a body in motion or a ray of light may be defined (as in figure 4b but strictly this can only be done within a local frame). In this context "continuous" means that the time between synchronous slices is less than the period of wave motion. The "time between slices" is not a precise quantity, but is a measure of the accuracy of measurement. In practice measurement accuracy is not well represented by a foliation, since measurement is more precise near the origin than at a distance from it. Doppler at frequency f defines a distance scale c/f . The effective Doppler rate as encoded onto the Pioneer S-band carrier signal is 1MHz giving a distance scale of 300m. When measurement accuracy is better than c/f the period of the signal is greater than the time between slices, and it is to be expected that Doppler will measure the mean, or geodesic, path over several slices as illustrated in fig-

ure 4b, yielding the standard general relativistic result. But when measurement accuracy is worse than c/f , a shift will be measured determining the apparent velocity between slices, yielding the illusory Pioneer acceleration. For measurement accuracy close to c/f the result is expected to be “noisy”. It appears difficult to separate this kind of noise from that due to solar radiation pressure.

On Earth we can make direct measurements of time using the counting frequency, or output, of atomic clocks at 5MHz. In practice, we can interpolate between this time period and the distance scale is effectively defined by the classical properties of solid matter and appears continuous on scales such that quantum effects may be ignored (in the orthodox interpretation it is not possible to discuss position as an empirical property except in an eigenstate of position). The Viking missions permitting ranging measurements of Mars to an accuracy typically quoted as 5-10m (Anderson quotes 12m), but ranging becomes increasingly difficult at larger distances and was not viable for Pioneer at the distance when the anomalous blueshift was first detected.

The discrepancy between real and illusory motion is accounted for by apparent jumps in the motion as illustrated by figure 4b. It is not clear whether such jumps are present in the original Pioneer data, since, if they appear, they may be treated as corrupted data and edited out from the analysis. As Anderson states: “there are inevitable problems that occur in data collection and processing that corrupt the data. So, at various stages of the signal processing one must remove or “edit” corrupted data. Thus, the need arises for objective editing criteria. Procedures have been developed which attempt to excise corrupted data on the basis of objective criteria. There is always a temptation to eliminate data that is not well explained by existing models, to thereby “improve” the agreement between theory and experiment. Such an approach may, of course, eliminate the very data that would indicate deficiencies in the a priori model”. If the teleconnection is responsible for the anomalous blueshift then this may happen; in the absence of a theoretical model the jumps in the motion seen in fig 4b would be treated as erroneous data. It is not clear that these jumps will appear in the Pioneer tapes, because they are associated with collapse of the wave function due to measurement of position, and no direct measurement of position of Pioneer appears possible. To carry out a proper test of the model a new mission is required in which both ranging and Doppler measurements are possible for a craft on an escape trajectory beyond the orbit of Saturn.

7 Flattening of Galaxies’ Rotation Curves

Although the Pioneer shift is not a physical acceleration it appears in a measurement of acceleration. What one actually measures is a shift in the momentum space wave function for each detected photon. This is a shift in an eigenstate, not a shift in the eigenvalue; notwithstanding this shift, the classical value of momentum is unchanged for Pioneer and the shift is described as an illusory momentum. For Pioneer there is a drift in illusory momentum, interpreted as an illusory acceleration. For an orbiting star the illusory momentum corresponds to an illusory increase in orbital velocity, which will be interpreted as illusory acceleration toward the galactic centre. This is present in the observation of distant galaxies and of the Milky Way, and accounts for flattening of galaxies’ rotation curves consistent with MOND, the phenomenological law proposed by Milgrom (1994) which retains Newton’s square law for accelerations $\ddot{r} \gg a_M$ for some constant a_M but replaces it with

$$\ddot{r} = -(GMa_M)^{1/2}/r \text{ for } \ddot{r} \ll a_M, \quad (7.1)$$

and gives a good match with data (a review of MOND is given by Sanders & McGaugh, 2002). According to the teleconnection this is an optical effect arising from the treatment of redshift, not a change to Newtonian dynamics or evidence of cold dark matter haloes. The accelerations

of galaxies in clusters are in the MONDian regime, and after revising the age-redshift relation, offer no immediate evidence that CDM is necessary to explain galaxy evolution.

The MOND test is particularly important for several reasons. Firstly, data fits have been given for over one hundred galaxies and for thousands of stars, secondly, because cold dark matter does not give any explanation as to why the precisely same acceleration law should be found in galaxies of many sizes and types, thirdly, because halo profiles from evolutionary models and lensing are neither consistent with each other nor with those found from rotation curves, fourthly because there is no satisfactory theory of CDM in particle physics, and finally because if there were no flattening of galaxies' rotation curves it would refute the teleconnection as a 'no CDM' model. In the context of rotation curves the CDM model is further distressed by the dynamical studies of three elliptical galaxies based on the measurement of radial velocities of a large number of planetary nebulae by Romanowsky et al. (2003). They find evidence for "little if any dark matter in these galaxies" and conclude that this does not naturally conform with the CDM paradigm.

Set up locally Minkowski coordinates with an origin at a galactic centre G with the galaxy in the xy -plane. For a star, S, at distance r from G and with an angular velocity ω about G, Pioneer blueshift is equivalent to an eigenstate of acceleration towards G of magnitude $Hc/2 = -a_p + \beta r \omega_p^2$, where a_p is the illusory Pioneer acceleration, ω_p is an illusory shift in angular momentum, and β is a factor required by quantum coordinates. For a star in a circular orbit $a_p = 0$. Let the shift in the eigenstate of orbital velocity be $v_p = r \omega_p$ so that $\beta v_p^2/r = Hc/2$, and let v_g be the true orbital velocity due to Newtonian gravity. Then the shifted orbital velocity is $v = v_g + v_p$.

Quantum coordinates with metric given by (3.2) are stretched in time by a factor of 2 and in the transverse direction by a factor of 1/2. So the blueshift corresponding to v_p is subject to a factor of 1/4 so that $\beta = 16$. First consider an idealised galaxy of zero mass (or an isolated star near an arbitrary point G). If the corresponding Doppler shift is interpreted as being due to the motion of a body in orbit about G with orbital velocity v_p then

$$\frac{v_p^2}{r} = \frac{H_0 c}{32} \text{ or } v_p = \pm \sqrt{\frac{H_0 c r}{32}}. \quad (7.2)$$

The velocity shift v_p is not directly observable, since if an observer on earth detects a photon from S then quantum coordinates must be used with S or the Earth at the origin. Now consider a massive Galaxy. The shifted orbital velocity is

$$v = v_g + v_p = \pm \sqrt{\frac{GM}{r}} \pm \sqrt{\frac{H_0 c r}{32}}. \quad (7.3)$$

And the shifted acceleration toward G is

$$\frac{v^2}{r} = \frac{GM}{r^2} + \frac{\sqrt{GMH_0 c/8}}{r} + \frac{H_0 c}{32}. \quad (7.4)$$

The last term is the shifted acceleration (7.2), which is removed when S is the source of a photon detected at the Earth, leaving a shift equivalent to acceleration:

$$\frac{v^2}{r} = \frac{GM}{r^2} + \frac{\sqrt{GMH_0 c/8}}{r}. \quad (7.5)$$

The first term on the right hand side of (7.4) is acceleration due to gravity. The second is an apparent inverse law acceleration in agreement with MOND. Thus $a_M = H_0 c/8$. The best fit value of a_M from observations on over a thousand stars is $1 \times 10^{-8} \text{ cm s}^{-2}$, consistent with recent determinations of Hubble's constant and with the value of $H_0 c$ given by Pioneer.

(7.5) applies to the Milky way as well as to distant galaxies and contributes an apparent motion of about 61 km s^{-1} to the measured orbital velocity of the Sun and local stars (figure 7). The same apparent orbital velocity is expected whenever wave effects are used to measure orbital velocity, whether by using VLBI to measure the proper motion of Sgr A*, or, more traditionally, by measuring the Doppler shift of Globular Clusters. According to (7.5) there is no MONDian interpolation function between the regimes $r \ll a_M$, in which the Newtonian inverse square law dominates, and $r \gg a_M$, where the MONDian inverse law has been found. As a result the predicted accelerations are larger than those predicted by MOND in the region $r \sim a_M$. An interpolation function gives a less good fit than that shown in figure 7 and in studies on globular clusters by Scarpa et al (2006) the flattening was observed at values of r up to $2.1 \pm 0.5 \times 10^{-8} \text{ cm s}^{-2}$. It is also notable that, to obtain fits with MOND for a number of low surface brightness galaxies, de Blok & McGaugh (1998) adjusted the inclination so as to increase accelerations in the region of the interpolation function. These fits have not yet been recalculated.

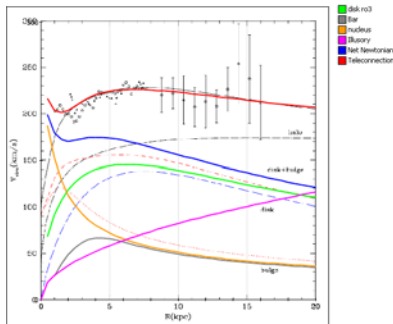


Figure 7: The teleconnection rotation curve for the Milky Way using a three part mass model described by Klypin, Zhao and Somerville (2002), superimposed on their model A₁, the “favoured” Λ CDM model. The fit is not optimised and uses the “user friendly” analytic approximation (eq10), with parameters close to those of model A₂, the Maximal Disk model, with disk scale length 3.5, $M_1 = 5.9 \times 10^{10}$, $M_2 = 4.8 \times 10^9$, $M_3 = 7 \times 10^9$. The rotation curve has been approximated by treating the mass internal to a given radius as a point source at the centre.

The illusory velocity contributes little to measured radial velocities for population I stars local to the sun. Figure 8 shows the full Doppler and the illusory element of the radial component of orbital velocity for Stars on diameters close to the sun assuming circular orbits. The observed illusory velocity is less than 0.5 km s^{-1} for a star with an orbit within 100pc of the solar orbit. Of possibly greater significance, an illusory orbital velocity of 61 km s^{-1} will contribute a systematic error in the order of 1mas to parallax, close to the accuracy of Hipparcos for individual stars and an order of magnitude greater than known systematic errors. It remains to analyse whether this will resolve the discrepancies between Hipparcos parallax distances to certain open clusters such as the Pleiades, and distances derived by other methods (Narayanan and Gould and references cited therein).

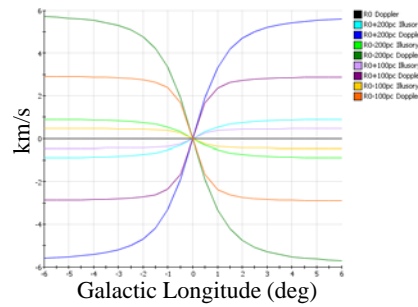


Figure 8: The full and the illusory component of radial velocity as measured by Doppler for stars in the vicinity of the Sun

As with the Pioneer shift the discrepancy between apparent and true velocities is taken up by apparent jumps in motion. It is possible, but by no means certain, that such a jump has already been observed. Ransom and Lebach (....) report that “Continuum VLBI observations at 3.6 cm of the RS CVn binary star IM Pegasi (HR 8703) for ~16 hr beginning on 1997 January 16 revealed an apparent motion of the star's radio position ... about two-thirds the estimated angular diameter of the primary component of the binary”. This is not the only instance of such a jump in the motion of IM Pegasi. In private correspondence Daniel Lebach wrote “In support of NASA's Gravity Probe B mission, we had 35 sessions of VLBI observations of IM Pegasi between 1997 and 2005. In 19 of these sessions the radio emissions from

the star were sufficiently bright that we could attempt to track apparent motions of the emissions. We marginally detected apparent motions in perhaps another three or four of these 19 sessions, but in none of the other sessions was the motion as pronounced or clearly apparent as in the session described in our ApJ. Lett. paper". Preliminary results have been placed on line (Ransom & Lebach, 2006) but data for analysis is not currently available. The target date for publication is April 2007. The researchers emphasise that they have other, very plausible, explanations for the results which cannot be eliminated, but if the teleconnection is correct it is hoped to correct these jumps to a real motion when complete data for the motions becomes available.

Two new space missions are scheduled for launch, Gaia by the ESA in 2011 and SIM Planetquest by JPL in 2015 (depending on budgetary approval). These will plot the positions and motions of stars in the Milky Way with unprecedented accuracy. It is hoped that this will provide a rigorous test of the model. It may ultimately be possible to detect a MONDian shift in Doppler in the inner solar system, but probably not at the effective frequencies used in Doppler navigation systems. Frequencies above 5MHz may hit engineering constraints since this is the counted frequency of an atomic clock. The shift should be present in optical frequencies in measurement of Mars, but at an amplitude two orders of magnitude lower than can be detected by HIRES, the high resolution echelle spectrometer in operation on the Keck Telescope. The equivalent orbital velocities are 1.8ms^{-2} for the Earth, 2.2ms^{-1} for Mars and 1.5ms^{-1} for Venus and the maximum contribution to Doppler shift is 0.34ms^{-1} for Mars, 0.23ms^{-1} for Venus, 1ms^{-1} for Jupiter and 1.23ms^{-1} for Saturn.

9 Big Bang Nucleosynthesis and CBR

The square law applies when all the information about the initial state is contained in the detected light, as in the observation of astronomical bodies. The cosmological microwave background is continuously observable. This scales coordinates as in figure 4b, and the standard linear red shift law applies. The analyses of big bang nucleosynthesis and of decoupling are unaltered, but the density of baryonic matter becomes $0.064 \leq \Omega_{\text{B}} h^2 \leq 0.096$ after normalising Ω_{cr} to 1 according to (5.2). Thus baryonic matter forms 10-20% of critical density. For $\Omega = 1.9$ the ratio of non-baryonic to baryonic matter need only be 9:1, and, after taking into account the redshift-age relation, the prospect remains open that this is might be accounted for by a massive neutrino.

The concordance model is supported by the integrated Sachs-Wolfe effect (Afshordi, Loh & Strauss; 2004; Boughn & Crittendon, 2004; Fosalba et al., 2003; Nolta et al., 2004; Scranton et al., 2004) using evidence from the Two-Degree Field Galaxy Redshift Survey (2dFGRS; Peacock et al. 2001; Percival et al., 2001; Efstathiou, 2002), and from the Wilkinson Microwave Anisotropy Probe (WMAP; Spergal, 2003, and references cited therein). In practice these measurements determine cosmological parameters rather than test consistency, and they depend on the distance-redshift relation. Acceleration depends only on distance and time, so that, if the standard model is consistent, a change in the distance-redshift relation can be expected to give a consistent change in the deceleration parameter in different tests in which distance is found from redshift. Thus it is to be expected that $\Omega_{\text{s}} \approx 0.3$ corresponds to $\Omega \approx 1.9$ in the teleconnection model whether it is determined from Supernova or from WMAP and 2dFGRS.

The broad properties of the microwave background are unchanged in the teleconnection model, as we expect isotropy and a gaussian random distribution, but it is not possible to interpret the WMAP data as implying that $\Omega_k = 0$, since this may be an artifact of quantum coordinates. McGaugh (2000) has shown that the low amplitude of the second peak in the Boomerang and WMAP data is consistent with a no CDM universe. Spergal comments on dis-

crepancies in the WMAP data on both the largest and smallest scales, and Copi et al (2006) report on unexplained alignments in the data. The same authors conclude their report on the year 1-3 data “At the moment it is difficult to construct a single coherent narrative of the low microwave background observations. What is clear is that, despite the work that remains to be done understanding the origin of the observed statistically anisotropic microwave fluctuations, there are problems looming at large angles for standard inflationary cosmology”. It is not presently possible to say whether these problems will be resolved by the teleconnection.

Acknowledgements

Thanks are due to Erik Anderson for figures 1 to 5 and for discussions on the manuscript, to Oz Hotz de Baar and Philip Helbig for discussions and comments on the manuscript, to Michelle Doherty for advice on the interpretation of extremely red objects and galaxy ageing, and to Peter Francis for his support during the research.

References

- Afshordi N., Loh Y.-S., Strauss M. S., 2004, *Phys. Rev.* **D69**, 083524.
- Anderson J. D., Laing P. A., Lau E. L., Liu A. S., Nieto M. M., Turyshev S. G., 2002, Study of the Anomalous Acceleration of Pioneer 10 and 11, *Phys.Rev.* **D65**, 082004.
- Arcos H. I., Pereira J. G., 2004, *Int.J.Mod.Phys.* D13 2193-2240.
- Astier P. et al., 2005, The Supernova Legacy Survey: Measurement of Ω_M , Ω_Λ and w from the First Year Data Set, accepted in A&A, astro-ph/0510447.
- Benitez N. et al, 2002, *Ap.J.*, **577**, L1-L4.
- Biviano A. & Salucci P., The radial profiles of the different mass components in galaxy clusters accepted in A&A. astro-ph/0511309.
- Boughn S. & Crittendon, 2004, *Nature* 427, 45.
- Cimatti. et. al., 2004, Old Galaxies in the Young Universe, *Nature*, **430**, 184-188.
- Copi C. J., Huterer D., Schwarz D., Starkman G. D., 2006, *MNRAS*, **367**, 79-102.
- de Blok, W.J.G., Bosma, A., & McGaugh, S.S. 2003, *MNRAS*, **340**, 657.
- de Blok, W.J.G., & McGaugh, S.S. 1998, *ApJ*, **508**, 132
- D’Inverno R., 1992, *Introducing Einstein’s Relativity*, Clarendon Press, Oxford.
- Doherty M., Bunker A. J., Ellis R. S., McCarthy P. J., 2005, *MNRAS*, **361** 525-549.
- Efstathiou G., et. al., 2002, *MNRAS*, **330**, L29.
- Einstein A., 1930, Auf die Riemann-metric und den Fern-Parallelismus gegründete einheitliche Field-Theorie, *Math Ann.*, **102**, 658-697.
- Eppley & Hannah, 1977, *Found. Phys.*, **7**, 51.
- Filippenko A. (2003), *Carnegie Observatories Astrophysics Series, Vol. 2: Measuring and Modeling the Universe*, ed. W. L. Freedman (CUP).
- Filippenko A. V., 2004, Type Ia Supernova and Cosmology, *White Dwarfs: Probes of Galactic Structure and Cosmology*, ed. E. M. Sion, H. L. Shipman, and S. Vennes (Kluwer: Dordrecht).
- Fosalba P. et. al., 2003, *ApJ*, **b**, L89.
- Francis C., 2006, A Relational Quantum Theory Incorporating Gravity, gr-qc/0508077.
- Glazebrook K. et. al., 2004, *Nature*, **430**, 181-184.
- Klypin A, Zhao H., and Somerville R. S., 2002, *Ap. J.*, **573**, 597–613
- Knop R. A. et al., 2003, *Astrophys.J.* 598, 102, astro-ph/0309368.
- Martel. H. and Shapiro P. R., 2003, astro-ph/0305174
- McGaugh, S. S., 2000, *Ap.J.*, **541**, L33-L36.
- McGaugh, S. S., 2004, *Ap.J.* **611**, 26-39.
- Mullis, P. Rosati, G. Lamer, H. Boehringer, A. Schwobe, P. Schuecker, R. Fassbender, 2005, Discovery of an X-ray-Luminous Galaxy Cluster at $z=1.4$, *ApJ Letters*, **623**, L85-L88.

- Milgrom M., 1994, *Ann. Phys.*, (NY) **229**, 384 Also see astro-ph/0112069.
- Milgrom M., Sanders R.H., 2005, *MNRAS*, **357**, 45-48.
- Misner C. W., Thorpe K. S., Wheeler J. A., 1973, *Gravitation*, Freeman, San Francisco.
- Mörtsell E., Gunnarsson C., Goobar A., 2001, *ApJ*, 561, 106.
- Narayanan V. K., Gould A., 1999, *Astrophys. J.*, **523**, 328-339
- Navarro, J. F., Frenk, C. S., & White, S. D. M. 1997, *ApJ*, **490**, 493.
- Nieto M. M., Turyshev S. G., 2004, *Class.Quant.Grav.* **21**, 4005-4024.
- Nolta M. R. et al., 2004, *ApJ*, **608**, 10.
- Park Y., Ferguson H. C., 2003, *Ap.J.* **589**, L65-L68, astro-ph/0304317
- Peacock J. A. et al., 2001, *Nature*, **410**, 169.
- Power C., Navarro. J. F., Jenkins A., Frenk C. S., White S. D. M., Springel V., Stadel J. and Quinn T., 2003, *MNRAS* **338**, 14-34, astro-ph/0201544
- Percival W. et al. 2001, *MNRAS*, **327**, 1297.
- Ransom R. & Lebach D., *Astrophys. J.*, **517**, Issue 1, pp. L43-L46
- Ransom R. & Lebach D., 2006, Preliminary Results, <http://aries.phys.yorku.ca/~ransom/results.html>
- Riess A. G et al, 2004, *Astrophys.J.*, **607**, 665-687.
- Romanowsky A.J., Douglas N.G., Arnaboldi M., Kuijken K., Merrifield M.R., Napolitano N.R., Capaccioli M., & Freeman K.C., 2003, *Science*, 301, 1696.
- Rovelli C., 2004, *Quantum Gravity*, CUP.
- Sanders R. H. & McGaugh S. S., 2002, *Ann. Rev. Astron. Astrophys.*, 40, 263-317.
- Scarpa R., Marconi G. & Gilmozzi R., 2006, *AIP Proceedings*, **822**, *Proceedings of the First Crisis in Cosmology Conference*, astro-ph/0601581.
- Scranton et al, 2004, *Physics Review Letters* astro-ph/0307335.
- Somerville R. S. et. al., 2004, *ApJ*, **600**, L135.
- Steigman G., 2005, to appear in *Int J. Mod.Phys. E*, astro-ph/0511534.
- Spergal D. L. et. al., 2003, *ApJS*, **148**, 175.
- Swaters, R.A., Madore, B.F., van den Bosch, F.C., & Balcells, M. 2003, *ApJ*, **583**, 732
- Toth V., Turyshev S. G., 2006, gr-qc/0603016.
- Turyshev S. G., Toth V. T., Kellogg L. R., Lau E. L., Lee K. J., 2006, *Int.J.Mod.Phys.* **D15**, 1-56.
- Wayth R. B., Warren S. J., Lewis G. F., Hewett P. C., 2005, *MNRAS*, **360**, 1333-1344.
- Zhao H, Bacon D. J., Taylor A. N., Horne I K., 2006, Testing Bekenstein's Relativistic MOND with Lensing, *MNRAS*. **368**, 171, astro-ph/0509590.

Appendix A Mathematical Description of the Teleconnection

A1 Coordinate Space

In an orthodox interpretation of quantum mechanics physical positions constituting a manifold are not meaningful between measurements. The teleconnection exploits this by using a metric, η , in the quantum theory which is not the physical metric, g , used in general relativity. The relationship between η and g is similar to that found by embedding of a manifold into a higher dimensional space, as described in some primitive accounts of general relativity. In this account the embedding space will have the same dimensionality as the embedded space. The method is a generalisation of the distinction between a cartographer's metric, i.e. the metric of the surface of the Earth, and a printer's metric, the metric of the paper which on which an atlas is printed. The use of an observer dependent, non-physical, metric for the quantum theory is legitimate for interpretations in which quantum theory is regarded as a method for calculating probabilities and not as a part of the physical description of matter; for example in the ortho-

dox, Dirac-Von Neumann interpretation, but not in a Copenhagen interpretation featuring Bohr's notion of complementarity.

Each local region, O , of a Lorentzian manifold, M , equipped with metric g , is considered as a subset, $U \subset \mathbb{R}^n$, together with a map, $\psi: U \rightarrow O$. Let U be denoted by axes $\alpha = 0, \dots, n$.

Definition: A coordinate space is any such subset $U \subset \mathbb{R}^n$ together with metric $\eta_{\alpha\beta}$.

Here $\eta_{\alpha\beta}$ is not the physical metric, g , but is an abstract metric used for mapping. Curvature is naturally conceived in terms of the scaling distortions of a map defined on coordinate space. In general straight lines in coordinate space are not geometrically straight, but for a sufficiently short line segment the deviation from straightness is not detectable, and, to first order, a short rod placed at x will appear as a small displacement vector, A^α , defined, as usual, as the difference in the coordinates of one end of the rod from the other. Coordinate space vectors will be defined by inverting the scaling distortions of the map such that for any physical vector, A , of magnitude m with metric g , the corresponding coordinate space vector, \bar{A} , will have magnitude m with metric η , i.e.

$$A^\alpha A^\beta g_{\alpha\beta} = \bar{A}^\alpha \bar{A}^\beta \eta_{\alpha\beta} = m^2 \quad (\text{A1.1})$$

Clearly \bar{A} is coordinate space dependent. For a unique definition of teleparallel displacement it is necessary to choose particular coordinates. *Quantum coordinates* will be determined in a natural manner in sections 2 and A3 by requiring plane wave motions in a homogeneous, isotropic cosmology. This will require metric (3.2) and yield a unique definition of teleparallel displacement. In general we can define orthogonal tetrads (or vierbein) such that the barred quantities are components in a local frame:

Definition: For each point $x \in U$, choose primed locally Minkowski coordinates with an origin at x , and define the matrix

$$\kappa^\alpha_\beta(x) \equiv x^{\alpha'}_\beta(x). \quad (\text{A1.2})$$

κ is defined using different primed locally Minkowski coordinates for each origin x , so that (A1.2) applies pointwise; it is written as an identity to show that it does not yield a differential equation. κ is not unique under this definition, and depends upon the choice of primed locally Minkowski coordinates at each point x ; for a Lorentzian manifold we may choose locally Minkowski coordinates at each point such that κ is differentiable.

Definition: For the vector, A^α , at position x , the corresponding coordinate space vector, barred to distinguish it from an ordinary, or physical, vector, is defined by

$$\bar{A}^\alpha(x) \equiv \kappa^\alpha_\beta(x) A^\beta(x). \quad (\text{A1.3})$$

This ensures that the coefficients of a coordinate space vector are equal to the coefficients of the corresponding vector in the primed, Minkowski, coordinates and preserves the inner product:

$$\eta_{\mu\nu} \bar{A}^\mu \bar{B}^\nu = \eta_{\mu\nu} \kappa^\mu_\alpha(x) \kappa^\nu_\beta(x) A^\alpha B^\beta = \eta_{\mu'\nu'} x^{\mu'}_\alpha(x) x^{\nu'}_\beta(x) A^\alpha B^\beta = g_{\alpha\beta}(x) A^\alpha B^\beta \quad (\text{A1.4})$$

(A1.4) is true for any vectors A^α , B^α . So

$$g_{\alpha\beta}(x) = \eta_{\mu\nu} \kappa^\mu_\alpha(x) \kappa^\nu_\beta(x). \quad (\text{A1.5})$$

(A1.5) gives the physical metric in terms of the variable scale coefficients, $\kappa^\mu_\alpha(x)$, of coordinate space vectors compared to physical vectors. Substituting (A1.2) into (A1.5) is a statement that locally Minkowski coordinates can be defined with an origin at any point, x , not that space is flat because different primed coordinates are associated with each origin. For the space-time coordinate, x , the coordinate space vector, \bar{x} generalises a displacement vector:

Definition: For any space-time coordinate (t, x) the coordinate space vector, $\bar{x} = (\bar{t}, \bar{x})$, is defined such that in locally Minkowski coordinate at the origin $\bar{t} = t$ and $\bar{x} = x$.

A2 Teleparallel Displacement

A short rod placed at x is described by vector, $A(x)$. An identical short rod is placed at y , so that its coordinate space vector is parallel to $\bar{A}(x)$. It is described by a vector, $A(y)$, whose length is unchanged, $A^2(x) = A^2(y)$.

Definition: $A(y)$ is teleparallel to $A(x)$ if and only if the coordinate space components are equal,

$$\kappa_{\beta}^{\alpha}(y)A^{\beta}(y) = \bar{A}^{\alpha}(y) = \bar{A}^{\alpha}(x) = \kappa_{\beta}^{\alpha}(x)A^{\beta}(x). \quad (\text{A2.1})$$

If coordinate space is tangent to local Minkowski space at x , axes can be chosen such that $\kappa_{\beta}^{\alpha}(x) = \delta_{\beta}^{\alpha}$ and (A2.1) reduces to

$$\kappa_{\beta}^{\alpha}(y)A^{\beta}(y) = \bar{A}^{\alpha}(y) = \bar{A}^{\alpha}(x) = A^{\alpha}(x) \quad (\text{A2.2})$$

Multiply both sides of (A2.2) by $\eta_{\alpha\gamma}\kappa_{\mu}^{\gamma}(y)$ and use (A1.5):

$$A_{\mu}(y) = A^{\alpha}(x)\eta_{\alpha\gamma}\kappa_{\mu}^{\gamma}(y) = A_{\gamma}(x)\kappa_{\mu}^{\gamma}(y). \quad (\text{A2.3})$$

A3 Quantum Coordinates

For a homogeneous isotropic cosmology it is natural to define coordinates using a foliation of space-like hypersurfaces which are spherically symmetric about any point. The quantum state is defined on a hypersurface of constant cosmic time. *Quantum coordinates* are defined by requiring that plane wave motions may be defined (at least in radial directions) such that momentum is always teleparallel to momentum observed at the origin.

Definition: In quantum coordinates the plane wave state, $|\bar{p}\rangle$, is defined at any location using coordinate space 4-vectors, $\bar{p} \equiv (\bar{E}, \bar{p})$ and $\bar{x} \equiv (\bar{t}, \bar{x})$. Then, at time $x^0 = t$,

$$\langle \bar{x} | \bar{p} \rangle = \langle \bar{t}, \bar{x} | \bar{p} \rangle = \left(\frac{1}{2\pi}\right)^{3/2} e^{-i(\bar{E}\bar{t} - \bar{x} \cdot \bar{p})} = \left(\frac{1}{2\pi}\right)^{3/2} e^{-i\bar{x} \cdot \bar{p}}. \quad (\text{A3.1})$$

This definition replaces the affine connection of classical general relativity in the quantum domain. It preserves Newton's first law and the constancy of the speed of light in quantum coordinates. In general teleparallel displacement requires flat coordinate space, but, for light emitted from a distant object at time t and detected at time t_0 , we merely require flatness in the time-radial plane. If we require spherical symmetry then, for some function, $g: \mathbb{R} \rightarrow \mathbb{R}$, and for some $b \in \mathbb{R}$ the coordinate space metric, η , is

$$ds^2 = b^2(d\tau^2 - d\rho^2) - g^2(\rho)(d\theta^2 + \sin^2\theta d\phi^2). \quad (\text{A3.2})$$

An FRW cosmology can be written in conformally flat coordinates, so that for $a = a(t)$ with $a_0 = a(t_0)$ the metric is

$$ds^2 = \frac{a^2}{a_0^2}(d\tau^2 - d\rho^2 - f^2(\rho)(d\theta^2 + \sin^2\theta d\phi^2)). \quad (\text{A3.3})$$

where the radial coordinate is $r = f(\rho) = \sin\rho, \rho, \sinh\rho$ for a space of positive, zero, or negative curvature respectively, and coordinate time, τ , is related to cosmic time, t , by

$$d\tau = \frac{a_0}{a} dt. \quad (\text{A3.4})$$

Then, for an FRW cosmology in coordinate space given by (A3.2), to first order near the origin, the coordinate space vectors are:

$$\bar{d}t = \frac{1}{b} dt, \quad \bar{d}r = \frac{a}{ba_0} dr, \quad \bar{d}\theta = \frac{f}{g} d\theta, \quad \bar{d}\phi = \frac{f}{g} d\phi. \quad (\text{A3.5})$$

A4 Classical Motion

Theorem: In local coordinates with an origin at time $t = t_0$ and with metric

$$ds^2 = dt^2 - dr^2 - r^2(d\theta^2 + \sin^2\theta d\phi^2), \quad (\text{A4.1})$$

for light emitted at time $x^0 = t$ and detected at the origin at time t_0 , momentum is given by

$$\bar{P}_0(x) = -i\frac{a_0^2}{a^2}\bar{\partial}_0, \bar{P}_1(x) = -i\frac{a_0^2}{a^2}\bar{\partial}_1, \bar{P}_2 = \bar{P}_3 = 0. \quad (\text{A4.2})$$

Proof: Light from a distant object is not observable unless $\bar{P}_2 = \bar{P}_3 = 0$. Using (A1.3) and (A3.3), in quantum coordinates, momentum at the time of emission is

$$\bar{P}_0(x) = -i\frac{a_0}{a}\bar{\partial}_0, \bar{P}_1(x) = -i\frac{a_0}{a}\bar{\partial}_1. \quad (\text{A4.3})$$

(A4.2) follows immediately on teleparallel displacement to the origin.

Let k^γ_μ be the scale factors between Minkowski coordinate spaces at x and y , so that

$$k^\gamma_\mu(x) = \frac{a}{a_0}\kappa^\gamma_\mu(y). \quad (\text{A4.4})$$

Then, by (A2.3), parallel displacement from the point x at time $x^0 = t$ to y at time $y^0 = t_0$ yields

$$A_\mu(y) = \frac{a}{a_0}A_\gamma(x)k^\gamma_\mu(y). \quad (\text{A4.5})$$

This result appears at first to be at odds with the claim that parallel displacement reduces to parallel transport in the classical correspondence. There is only an issue concerning cosmological redshift - gravitational redshift is not altered. The resolution lies in the manner in which expansion is treated in the quantum theory. The quantum state is defined on a synchronous slice using cosmic time as described in figure 4b; (A4.2) applies in the quantum theory between initial and final states. In order to describe a continuous classical motion we must treat a collection of synchronous slices, and treat each slice as the final state of one quantum step and as the initial state of the next quantum step, then allow the step size to go to zero, to obtain a foliation. Thus the motion is described as a sequence of states $|f(t_i)\rangle$ at instances $t_i \in T$ with $0 < t_i - t_i < \chi$ in the limit as χ tends to zero. Momentum is parallel displaced in each coordinate space using (A4.2). Due to cosmological expansion, the size of the slice changes between considering it for a final state and for an initial state. This means we have to rescale coordinates to the torus $(-\pi, \pi)^3$ and consequently renormalise momentum between one quantum step and the next, thereby removing a factor a/a_0 . Thus, (A4.2) is replaced by

$$P_0(x) = -i\frac{a_0}{a}\partial_0, P_1(x) = -i\frac{a_0}{a}\partial_1, P_2 = P_3 = 0. \quad (\text{A4.6})$$

and (A4.5) gives

$$P_\mu(y) = P_\gamma(x)k^\gamma_\mu(y). \quad (\text{A4.7})$$

When $y = x + dx$ (A4.7) is the standard formula for infinitesimal parallel displacement in a tangent space. The cumulative effect of such infinitesimal parallel displacements is parallel transport. So teleparallelism of momentum between initial and final states in quantum theory, together with renormalisation of momentum, gives rise to parallel transport in the classical domain. Geodesic motion of a classical particle follows as the cumulative effect of displacements in the direction of momentum over small time increments. The same argument holds for a classical beam of light, in which each photon wave function is localised within the beam at any time, and for a classical field which has a measurable value at each point where it is defined.